2

FTD-ID(RS)T-0260-88





# FOREIGN TECHNOLOGY DIVISION

BASIC RULES OF SATURATED GAIN VARIATION IN A FLOWING LASER CAVITY

by

Wu Zhongxiang, Yan Haixing

# HUMAN TRANSLATION

FTD-ID(RS)T-0260-88 8 July 1988

MICROFICHE NR: FTD-ID(RS)T-000536

BASIC RULES OF SATURATED GAIN VARIATION IN
A FLOWING LASER CAVITY

By: Wu Zhongxiang, Yan Haixing

English pages: 10

Source: Jiguang, Vol. 7, Nr. 3, 1980, pp. 5-8

Country of origin: China
Translated by: FLS, Inc.
F33657-85-D-2079
Requester: FTD/TQTD
Approved for public release; Distribution unlimited.

GRAPHICS DISCLAIMER

All figures, graphics, tables, equations, etc. merged into this translation were extracted from the best quality copy available.

# Basic Rules of Saturated Gain Variation in a Flowing Laser Cavity

by Wu Zhongxiang and Yan Haixing
(Institute of Mechanics, Academia Sinica)

Paper received on August 27, 1979.

**From numerical calculation, the basic rules of saturated gain coefficient variation with the field distribution along the flow direction in a Gas Dynamic Laser (GDL) cavity are presented. In connection with variations of vibrational energy and temperature of all modes, these rules are explained with the physical mechanism of relaxation of the active medium. It is pointed out that, for example, there still exists considerable vibrational energy which can be used for Gerry's device with 30 KW monomode output.**

[illegible]

## I. Preface

Under a certain light cavity structure condition, a stable distribution of a radiation field can be reached in consequence of compromising between its gain and loss (due to diffraction, loss, output, mirror absorption and so forth); the corresponding saturated gain distribution is thus obtained. The characteristics of laser output power, beam quality, etc. can then be determined.

The basic physical mechanism of a laser can be reflected through the saturated gain, the energy of each mode and the variation rules of vibrational temperature which changes along with the radiation field distribution (the flowing laser coordination is along the moving direction).

The importance of the saturated gain coefficient in a light cavity is beyond doubt; however, there is no concrete discussion and analysis about its variation rules in the current literature (only approximation formulae under a simplified condition are given in Ref. [1, 2, 6]). Based on a $CO_2$-$N_2$-$H_2O$ gasdynamics laser and a light cavity theoretical model [4], the paper presents the saturated gain distribution in a laser cavity by using a numerical method to solve a set of relaxation equations [3] and a propagation equation of a radiation field. An analysis of the variation rules of this saturated gain with the radiation field distribution in the cavity is also conducted.

## II. Method of Calculation

When a relaxation model named "three modes and four vibrational temperatures" [3] is adopted for a $CO_2$-$N_2$-$H_2O$ system, then a set of relaxation equations which describe the vibration of each mode along the flow direction (x) and a propagation equation of the cavity radiation field are solved simultaneously (using the calibrated Rensch interpolation scheme). Based on the assumption of "repeatedly increasing field strength", the total intensity of the propagating light which travels back and forth in the cavity is then calculated; then a stable distribution of the radiation field in the cavity as well as the vibrational energy, vibrational temperature and saturated gain of the active medium at each mode can be found.

Similar to the common approach, the flow speed, density and temperature in the cavity are assumed to be constants in order to simplify the problem, thus eliminating the coupling effect among these parameters and the radiation distribution, as well as the medium relaxation process. Since the vibrational energy of the active medium possesses only a small percentage of total enthalpy, and moreover only a small portion of this energy is dissipated into the flow and changes these parameters; therefore, effects of the vibration on them are not significant as long as the flow parameters in the cavity are uniformly distributed.

All of the relaxation data used in the calculation are self-collected and processed. Since the total light intensity at the upstream of the entrance is negligible, the gain coefficient at that location is equal to the small signal gain, and an equilibrium exists in between the initial upper energy level of $N_2$ and $CO_2$ lasers while the vibrational temperature at the lower energy level is in approximation to the translational temperature. Thus, all initial values are solved by using simple algebraic operations.

## III. Variation Rules of Saturated Gain

Similar to Rensch's method, the Gerry's "hollow vertical elongated cavity" model [4] is examined. This model has an unstable cavity in which the light is repeatedly reflected along the vertical direction in the "Z" shape and has been discussed by Locke et. al. [5] in detail. Results are listed in Table 1 and are also shown in the figures.

The figures show that a small signal gain (when total intensity $I \sim 0$) slowly and monotonically decreases following a negative exponential function along the flow direction. When $I \neq 0$ (the stable total intensity distribution inside the cavity is shown in Fig. 1), the variations of a saturated gain, $G(x)$, along the flow direction are different according to the differences of total intensity distribution $I(x)$, as shown in Fig. 2.

The basic variation rules are:

(1) In the area where I abruptly increases, $G(x)$ decreases dramatically with x.

(2) In the area where I basically is a constant, $G(x)$ monotonically decreases following a negative exponential function. Moreover, the decreasing slope increases when I increases.

(3) In the area where I abruptly decreases, G(x) increases correspondingly with x.

Table 1 Vibration temperature and gain distributions for both with and without radiation fields

| (1) 流动方向相对坐标 | $T_1$(K) | $T_I-T$ | $T_{II}$ | $T_{II}-T_3$ | $G_0$ (2) ($10^{-3}$ 厘米$^{-1}$) | $I$ (3) (瓦/厘米$^2$) | $T_1$(K) | $T_I-T$ | $T_{II}$ | $T_{II}-T_3$ | $G$ (4) ($10^{-3}$ 厘米$^{-1}$) |
|---|---|---|---|---|---|---|---|---|---|---|---|
| −50 | 333.36 | 2.30 | 1021.70 | 25.84 | 4.27 | 0 | 333.36 | 2.30 | 1021.70 | 25.84 | 4.27 |
| −40 | 337.70 | 6.64 | 1019.35 | 25.51 | 4.19 | 0 | 337.70 | 6.64 | 1019.35 | 25.51 | 4.19 |
| −30 | 339.43 | 8.36 | 1017.01 | 25.40 | 4.14 | 487 | 341.96 | 10.90 | 1016.59 | 35.65 | 3.97 |
| −25 | | | | | | 882 | 346.89 | 15.83 | 1014.12 | 47.24 | 3.69 |
| −20 | 340.09 | 9.03 | 1014.68 | 25.28 | 4.10 | 882 | 352.66 | 21.60 | 1008.81 | 54.03 | 3.45 |
| −10 | 340.33 | 9.27 | 1012.35 | 25.15 | 4.06 | 882 | 356.60 | 25.54 | 999.43 | 53.41 | 3.2[illegible] |
| 0 | 340.38 | 9.32 | 1010.04 | 25.03 | 4.03 | 882 | 357.62 | 26.56 | 990.23 | 52.23 | 3.16 |
| 10 | 340.36 | 9.30 | 1007.73 | 24.90 | 4.00 | 882 | 357.52 | 26.46 | 981.28 | 51.19 | 3.05 |
| 20 | 340.31 | 9.25 | 1005.44 | 24.78 | 3.47 | 882 | 356.49 | 25.93 | 972.39 | 50.21 | 2.95 |
| 25 | | | | | | 882 | 356.59 | 25.53 | 967.17 | 49.65 | 2.89 |
| 30 | 340.24 | 9.18 | 1003.15 | 24.65 | 3.93 | 487 | 355.20 | 24.14 | 962.90 | 43.13 | 2.94 |
| 40 | 340.18 | 9.12 | 1000.88 | 24.52 | 3.90 | 0 | 346.67 | 15.61 | 959.40 | 23.91 | 3.25 |
| 50 | 340.11 | 9.05 | 998.61 | 24.39 | 3.87 | 0 | 342.06 | 11.02 | 957.19 | 22.26 | 3.29 |

Key: (1) Relative coordinate along the flow direction; (2) 1/cm; (3) Watt/cm².

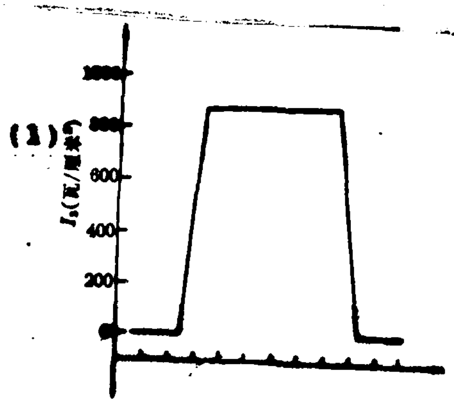


Fig. 1
Key: (1) Watt/cm².

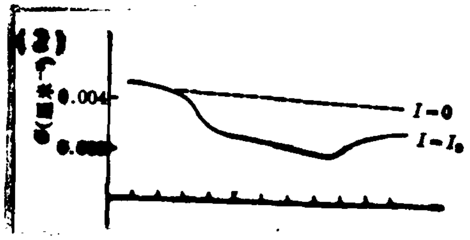


Fig. 2
Key: (1) 1/cm.

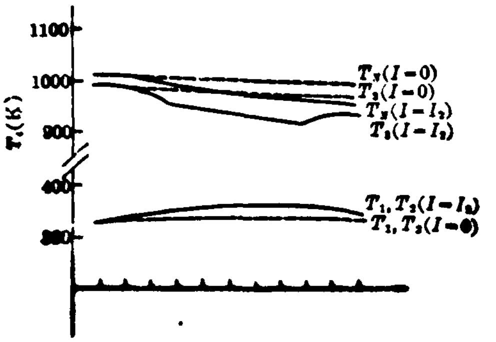


Fig. 3

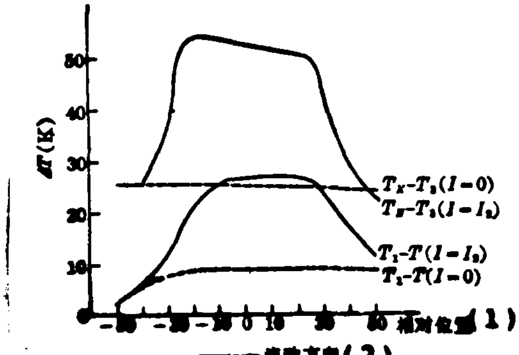


Fig. 4

Key: (1) Relative position
(2) Flow direction.

## IV. Physical Interpretations

In order to interpret the variation rules of the saturated gain stated above based on the physical mechanism of energy transfer inside a system, several parameters are calculated by adopting the "three modes and four vibrational temperatures" model. These parameters which include the relaxation energy transfer terms [3] and the radiation energy transfer terms [4] among the modes as well as their corresponding relaxation rates (the definition of the effective radiative relaxation rate, $\overline{\tau_v^{-1}}$, is described in Ref. [6]) are calculated and are listed in Table 2 and 3.

Table 2 Rates of various energy transfer processes

| $T=$[illegible]K, $P=$[illegible] 大气压(1) $X_c:X_N:X_H=$[illegible]:[illegible]:[illegible], 速率单位: 1/秒(2) | | | | |
|---|---|---|---|---|
| $\nu_N\to$平动 (3) | $\nu_3\to3\nu_2$ | $\nu_3\to\nu_N$ | $\overline{\tau_v^{-1}}$ ($I=487$ 瓦/厘米$^2$) (4) | $\overline{\tau_v^{-1}}$ ($I=$[illegible] 瓦/厘米$^2$) (4) |
| $1.6\times10^5$ | $1.4\times10^4$ | $4.9\times10^5$ | $4.0\times10^4$ | $7.1\times10^4$ |

Key: (1) Atm; (2) Rate unit: 1/sec; (3) Translation; (4) Watt/cm².

Table 3 Values of each energy transfer term at mirror center (Unit: I - Watt/cm²; Energy transfer term - Watt/cm )

| $I$ | $\left(\frac{dE_3}{dt}\right)_{\nu_3\to\nu_2}$ | $\left(\frac{dE_2}{dt}\right)_{\nu_3\to 3\nu_2}$ | $\left(\frac{dE_1}{dt}\right)$(1) | $\left(\frac{dE_2}{dt}\right)_{\nu_2\to T}$ |
|---|---|---|---|---|
| 0 | 2.2 | 1.9 | 0 | −2.0 |
| [illegible] | [illegible] | 1.6 | 4.3 | −8.7 |

Key: (1) Radiation.

Without a radiation field, $\nu_3\to 3\nu_2$ is the only case of an energy transfer process which consumes the upper level energy. Table 2 shows that its rate is much smaller than $\nu_3\to\nu_2$ of the supplying laser upper energy level and $\nu_2$ -- translation of the evacuated laser lower energy level. Therefore, as long as a smaller difference is maintained between $T_3$ and $T_N$ as well as between $T_1$ ($\sim T_2$) and T (see Table 1), a sufficient energy flow can be created to support the reverse (see Table 3). At this moment, the variation of $G_0$ is monotonically decreasing along the flow direction (see Fig. 2). The vibrational temperatures, $T_N$ (Fig. 3) and $T_N$-$T_3$ (Fig. 4), of $N_2$ which is a vibrational energy reservoir of the active medium are both monotonically decreasing.

With a radiation field, the situations are quite different. By consuming the $\nu_3$ vibration energy, the vibration energy of a composite mode $(\nu_1, \nu_2)$ can be increased simultaneously. In addition to the relaxation energy flow created during the V-V interchanging process, an energy flow created by radiation also increases. Table 2 indicates that the radiation energy transfer rate is much larger than the relaxation energy transfer rate. Moreover, this difference increases when the radiation field strength increases. The rate difference between the supplying upper energy level and the consuming upper energy level is noticeably reduced. This is especially true for the energy transfer rate at the evacuated low energy level. In order to maintain the energy flow balance, the differences between $T_1$ and T as well as $T_N$ and $T_3$ should be enlarged. This difference is more obvious in the areas which have a strong radiation field (as shown in Table 1 and Fig. 3, 4). In other words, in the area which has a strong radiation field, effects of the consuming upper energy level during the radiation process is greater than the relaxation process (see Table 3). The common effect of these two processes causes insufficient evacuation for the low energy level (increases of $T_1$ and $T_2$ are too much) and delay of the supply for the upper energy level (decrease of $T_3$ is too much, as shown in Fig. 3). However, the gain depends on the number of reversing particles at both upper and lower laser energy levels. In other words, this only depends on $T_3$ and $T_1$, and consequently, the saturated gain is over-reduced. Once the radiation field disappears, the processes of supplying an upper energy level as well as evacuating a lower energy level can return to a relatively high rate condition which makes the temperature difference between $T_N$-$T_3$ and T-$T_1$ correspondingly reduce (see Fig. 4). This means that $T_3$ correspondingly increases while $T_1$ correspondingly decreases (as shown in Fig. 3), and the saturated gain shows its recovery (see Table 1 and Fig. 2). However, the total vibrational energy in the $N_2$ energy reservoir is continuously consumed. The consuming rate is higher when a radiation field exists, even in the area where the radiation field is obviously reducing. From Table 1 and Fig. 3, $T_N$ always monotonically decreases (the decreasing rate is larger in the high radiation area).

## V. General Considerations

To evaluate an active medium, it is essential to examine the usable energy of the medium (for a $CO_2$-$N_2$-$H_2O$ system, mainly is $N_2$ vibrational energy) besides the magnitude of its gain.

From the results of calculation against one of Gerry's cavity models which has a "Z" shaped repeat reflection along the vertical direction, $N_2$ vibration temperature, $T_N$, at the upstream entrance is ~ 1200K, and it only drops to ~ 957K at the downstream exit; however, the vibrational temperature of a "no reverse" laser upper energy level is $\boxed{T_3 \approx \frac{\theta_3}{\theta_1} T}$, which is around 600K; therefore, there is a considerable amount of effective energy which is wasted. Moreover, the gain at the cavity exit can further pick up, and its gain value (% 1/cm) drops from 4.3 at entrance to 3.3 at exit. All of these indicate that in the active medium still exists a considerable amount of usable energy.

Of course, the calculated gain at exit and the effective energy may be on the high side because various nonuniformities (such as shock waves, tail flows, etc.) are ignored, and all flow parameters are considered as constants instead of coupling with the flow equations (#2 has made an estimation that this error will not be too large, if there is no serious nonuniformity inside the cavity). Nevertheless, this device still possesses a great development potential.

References:


[1] W. W. Rigrod; *J. Appl. Phys.*, 36, 8 (1965), 2487.

[2] A. E. Siegman; *Appl. Opt.*, 13, 12 (1974), 2775.

[3] 严海星, 陈丽吟;《力学学报》, 1978, No. 4, 274.

[4] D. B. Rensch; *Appl. Opt.*, 13, 11 (1974), 2546.

[5] E. V. Locke et al.; *IEEE J., Quant. Electr.*, QE-8(1972), [illegible].

[6] A. L. Hoffman et al.; *IEEE J., Quant. Electr.*, QE-8(1972), 46.

## DISTRIBUTION LIST

## DISTRIBUTION DIRECT TO RECIPIENT

| ORGANIZATION | MICROFICHE |
|---|---|
| A205 DMAHTC | 1 |
| A210 DMAAC | 1 |
| C509 BALLISTIC RES LAB | 1 |
| C510 R&T LABS/AVEADCOM | 1 |
| C513 ARRADCOM | 1 |
| C535 AVRADCOM/TSARCOM | 1 |
| C539 TRASANA | 1 |
| C591 FSTC | 4 |
| C619 MIA REDSTONE | 1 |
| D008 MISC | 1 |
| E053 HQ USAF/INET | 1 |
| E404 AEDC/DOF | 1 |
| E408 AFWL | 1 |
| E410 AD/IND | 1 |
| E429 SD/IND | 1 |
| P005 DOE/ISA/DDI | 1 |
| P050 CIA/OCR/ADD/SD | 2 |
| AFIT/LDE | 1 |
| FTD | |
| CCV | 1 |
| MIA/PHS | 1 |
| LLYL/CODE L-389 | 1 |
| NASA/NST-44 | 1 |
| NSA/T513/TDL | 2 |
| ASD/FTD/TQIA | 1 |
| FSL/NIX-3 | 1 |